CNRS

Centre National de la Recherche Scientifique

INFN

Istituto Nazionale di Fisica Nucleare

SEARCH FOR NOISE SOURCES IN C1 AND C2 SENSITIVITIES

VIR-NOT-LAP-1390-277

Raffaele FLAMINIO, Romain GOUATY, Edwige TOURNEFIER

Date : 05/08/2004

VIRGO * A joint CNRS-INFN Project
Project Office: VIRGO Traversa H di via Macerata-56021 S.Stefano a Macerata Cacina (Pisa) Italy.
Secretariat: Telephone.(39) 050 732 521 * FAX.(39) 050 752 550 * e-mail virgo@Pisa.infn.it

1. Introduction

Two commissioning runs with a simple Fabry-Perot cavity locked have been achieved since the beginning of VIRGO Commissioning (started at the end of the year 2003) : From November 14th to November 17th of 2003, C1 run permitted to collect a three days long set of data with North arm cavity locked. It was followed by C2 run from February 20th to February 23rd of 2004, during which linear automatic alignment was working on the North cavity, and the West cavity was locked for several hours for the first time.
The goal of this note is to list the predominant noise sources which have an impact on the C1 and C2 sensitivities.
The method used to search for noise sources consists first in looking for channels which are coherent with the dark fringe signal. Then, the second step consists in finding a model to propagate the noise through the interferometer.
In section **2**, the sensitivity curves obtained during C1 and C2 are presented. Some noise sources have been clearly identified and we are able to give a model to propagate them through the interferometer : These sources, ADC noise for highest frequencies and "laser frequency noise" for intermediate frequencies, are described in sections **3** and **4** respectively. The hypothesis on noise sources which are likely to explain the sensitivity during C2 between 150Hz and 3kHz are discussed in section **5**. For lowest frequencies, the sensitivity during C1 seems to be limited by angular motion noise as explained in section **6**. Finally, in section **7**, North arm and West arm sensitivities during C2 are compared.

2. Sensitivity curves during C1 and C2

The sensitivity is given by the amplitude spectrum of the dark fringe signal (Pr_B1_ACp or Pr_B1p_ACp) multiplied by the calibration transfer function (see http://wwwcascina.virgo.infn.it/DataAnalysis/Calibration/TF.html).
This transfer function is used to convert the dark fringe signal given in Watts to displacement signal in meters corrected from both the optical response and the locking system effect.
Figure 1 shows the two sensitivity curves obtained during C1 and C2 when North Cavity was locked. The C1 sensitivity is calculated from five minutes of data starting at GPS time = 753113490 (November 17th 2003, 14h10 UTC), and the C2 sensitivity from five minutes of data starting at GPS time = 761345400 (February 20th 2004, 20h50 UTC). In both cases, the dark fringe signal was taken after the Output Mode Cleaner (Pr_B1_ACp).
The differences between the two curves will be explained in the following.

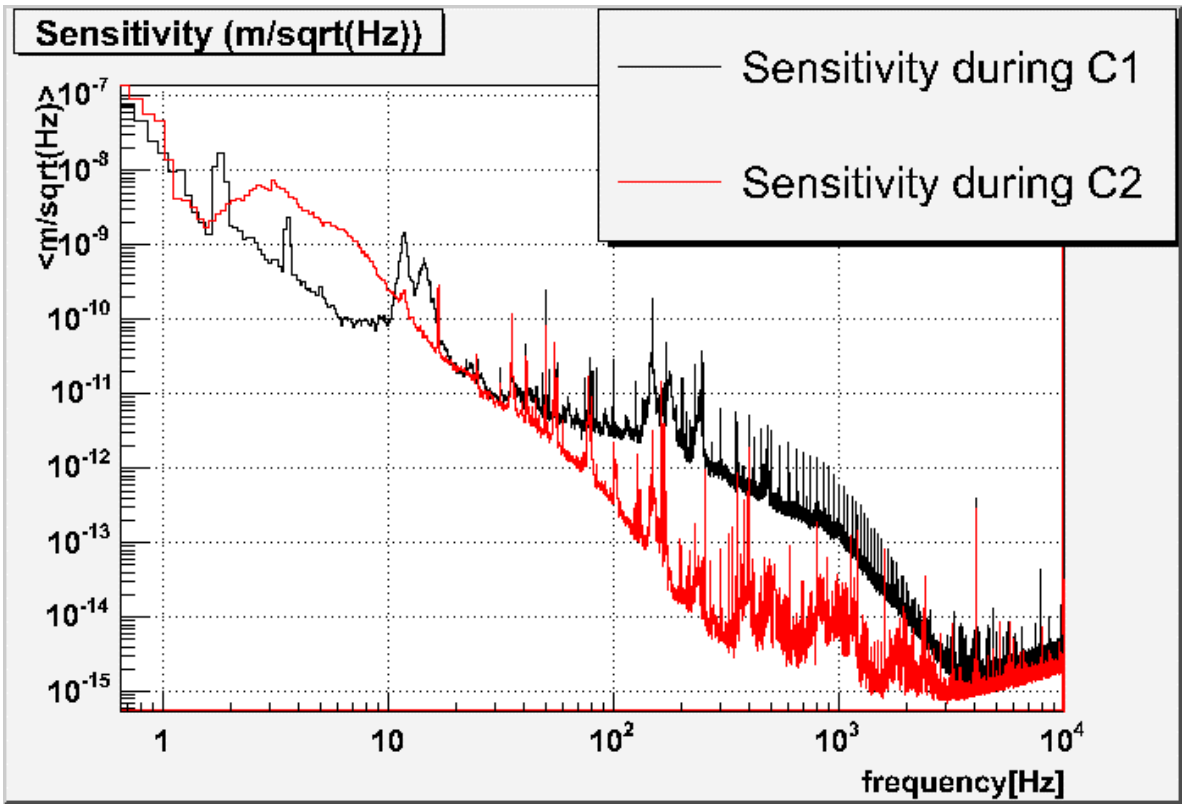

Figure 1 : *Sensitivity curves for C1 (black) and C2 (red)*

3. Electronic noise and shot noise

Electronic noise can be measured with channel Pr_B1_ACp when B1 shutter is closed (which guarantees that no light reaches the photodiode). Appropriate data are available for C1 run on Friday November 14th 2003, 14h50 UTC, and for C2 run on Friday February 20th 2004, 15h30 UTC.

Shot noise can be evaluated during the period used to plot the sensitivity curves thanks to the relation :

$$S_{sn} = \sqrt{2hnP_{DC}} \times \sqrt{2}$$

where : S_{sn} represents the shot noise level given in W/√Hz ;

h is the Planck's constant ;

n is the laser frequency ;

P_{DC} represents the mean DC power (in W) which reaches the photodiode ;

the factor $\ddot{O}2$ is due to the demodulation process.

Both electronic noise and shot noise are converted in m/√Hz by using the calibration transfer function. The result is shown on Figure 2 for C2 run.

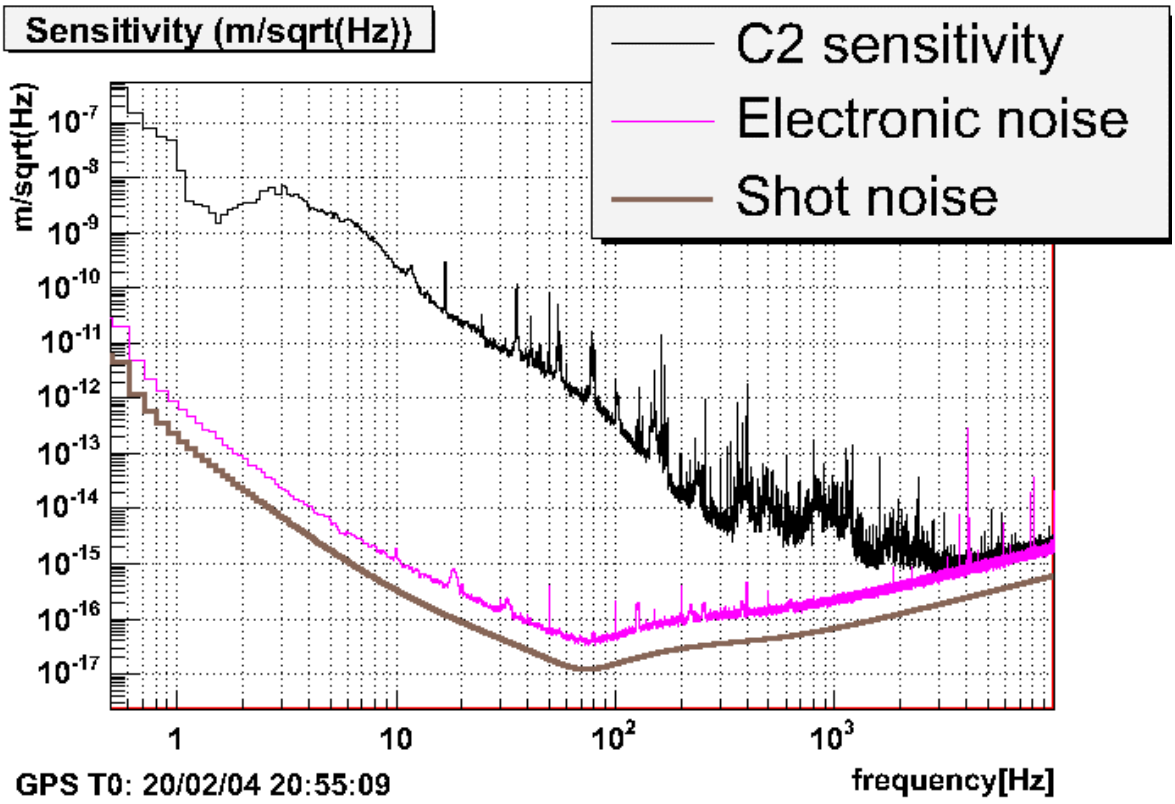

Figure 2 : *Electronic noise contribution in the sensitivity during C2*

One can observe that the sensitivity is dominated by electronic noise above 3 kHz. Shot noise level is still lower than electronic noise by a factor of five. Actually, the main contribution in the electronic noise was due to ADC. If electronic gains could have been increased, the contribution of ADC noise would have been reduced consequently. But, as noise was quite high at low frequencies, it was not possible to increase the gain, otherwise ADC dynamics would have been saturated.
The electronic noise contribution was exactly the same for C1 and C2 runs.

4. "Laser frequency noise"

As it will be shown latter, a good coherence is observed between the dark fringe signal Pr_B1_ACp and the signal measuring the "laser frequency noise". Thus, this kind of noise seems to be a relevant candidate to explain the sensitivity. Therefore, we have built models to propagate this noise through the interferometer. They are presented in the next section.

4.1. Models to propagate "Laser frequency noise" through the Interferometer

In this part, the notation *dX* refers to a fluctuation of the variable *X*, implicitly taken in the frequency domain.

"Laser frequency noise" can be understood by considering the consequences of a longitudinal displacement *dL* of the Input Mode Cleaner (IMC) end mirror. As it has been shown in [1], two effects are going to result from this displacement :

- First, since laser frequency is controlled by IMC length (see Figure 3), a longitudinal displacement of the IMC end mirror produces a drift in the laser frequency, *dn*, given by :

$$\frac{dn}{n} = -\frac{dL}{L_{IMC}},$$

where n is the laser frequency ($n = 2.82 \times 10^{14}$ *Hz*) and L_{IMC} the IMC cavity length ($L_{IMC} = 140$ *m*). The resulting frequency noise at the exit of IMC dn'_1 is obtained by the relation :

$$dn'_1 = \frac{dn}{1 + i\frac{f}{f_c}},$$

where *dn* has been multiplied by the IMC transfer function ($f_c = 500$ *Hz*).

- The second effect is due to the fact that the IMC length fluctuation modifies the phase of the beam resonating in IMC cavity. This phase fluctuation is equivalent to a frequency noise given, at the exit of IMC cavity, by :

$$dn'_2 = -i\frac{f}{f_c}\frac{dn}{1 + i\frac{f}{f_c}}$$

The addition of these two effects leads to :

$$|dn'| = |dn'_1 + dn'_2| = |dn| = \left|dL\frac{n}{L_{IMC}}\right| \qquad \textbf{(1)}$$

The frequency noise $|dn'|$ is then converted into m/√Hz :

$$dl = |dn'| \times \frac{L_{arm}}{n} = |dn| \times \frac{L_{arm}}{n} = |dL| \times \frac{L_{arm}}{L_{IMC}} \qquad \textbf{(2)}$$

where L_{arm} is the length of the north arm (or west arm) : $L_{arm} \approx 3 \times 10^3$ *m*.

Equation **(2)** gives the contribution in the sensitivity of any kind of IMC length fluctuations. Two different methods, which depend on the noise source, can be used to evaluate *dL* or *dn*. They are described in what follows.

a) IMC length noise

The laser frequency drift $|dn|$ is directly measured by the Reference Cavity reflection signal (Sc_IB_zErrGCx30 during C1 or Sc_IB_zErrGC during C2) if there is no readout noise in this channel. In this case, the resulting IMC length noise converted into m/√Hz is obtained from :

$$dl = FFT(Sc\_IB\_zErrGC(x30)) \times K_{V \to Hz} \times \frac{L_{arm}}{n} \qquad \textbf{(3)}$$

The symbol FFT is for the Fast Fourier Transform.

$K_{V®Hz}$ is a normalisation factor which converts the channel Sc_IB_zErrGC(x30) from Volts to Hertz.

b) IMC length control noise

If Sc_IB_zErrGC(x30) contains some readout noise, equation **(3)** does not work because this channel is no more relevant to evaluate laser frequency drift. In this case, the longitudinal displacement *dL* of the IMC end mirror results from the transmission of the readout noise by the IMC length control loop (see Figure 3), and can be evaluated from :

$$dL = FFT(Sc\_MC\_zCorrR) \times \frac{1}{f^2} \times K_{V \to m} \qquad \textbf{(4)}$$

Sc_MC_zCorrR is the correction signal sent to the IMC end mirror. Its spectrum has been multiplied in equation **(4)** by the pendulum mechanical transfer function ($1/f^2$). $K_{V®m}$ is a normalisation factor which converts the channel Sc_MC_zCorrR from Volts to displacements.

Finally, the contribution in the sensitivity of IMC length control noise is obtained from equation **(2)** by replacing *dL* by its expression given in **(4)** :

$$dl = FFT(Sc\_MC\_zCorrR) \times \frac{1}{f^2} \times K_{V \to m} \times \frac{L_{arm}}{L_{IMC}} \qquad \textbf{(5)}$$

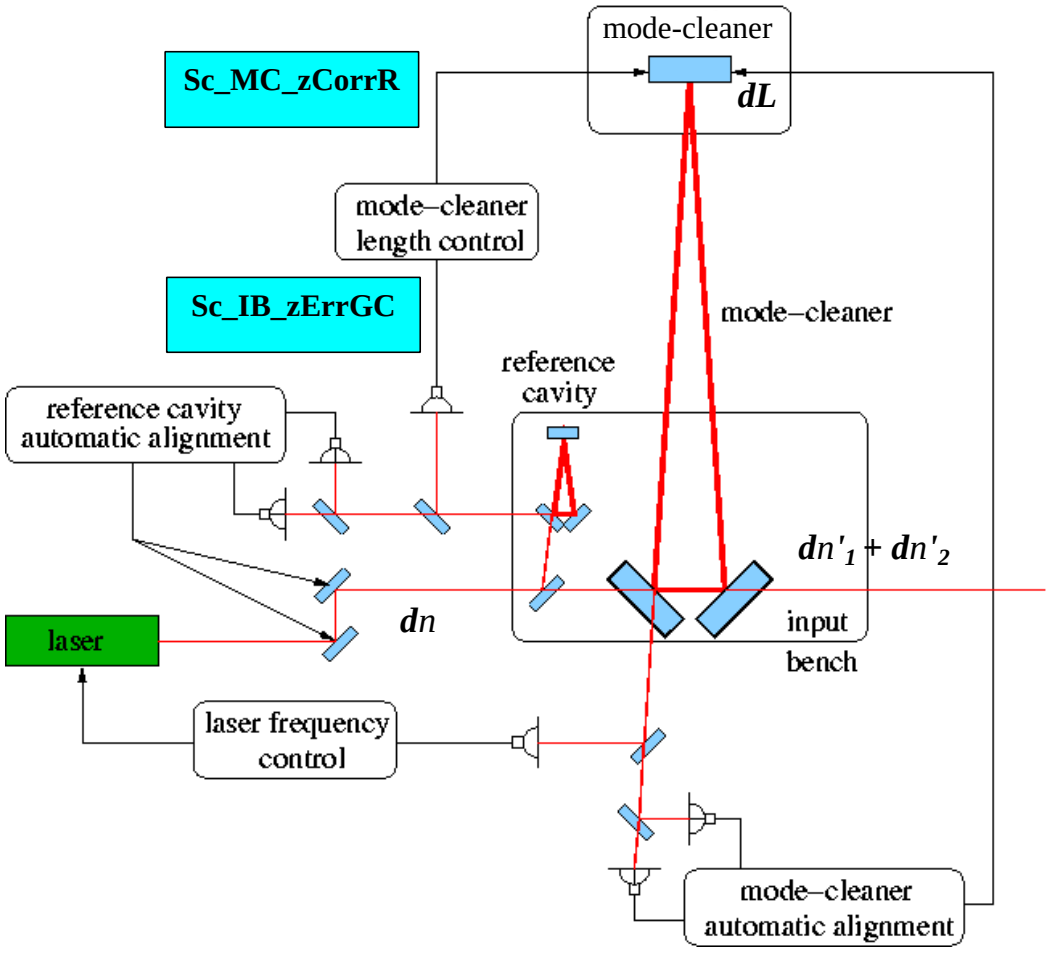

Figure 3 : *Schematization of the injection loops implied in "laser frequency noise"*

4.2. "Laser frequency" noise during C1

Figure 4 shows the coherence between the dark fringe signal (Pr_B1_ACp) and the Reference Cavity reflection signal (we took the channel Sc_IB_zErrGCx30 as channel Sc_IB_zErrGC was limited by electronic noise).

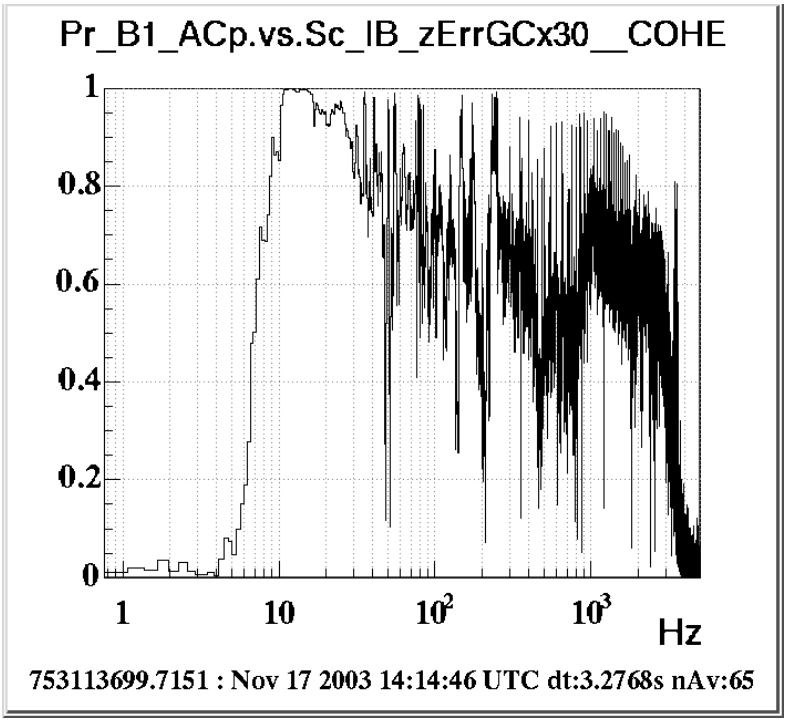

Figure 4 : *Coherence between Pr_B1_ACp and Sc_IB_zErrGCx30 during C1*

One can notice that the coherence is quite good between 10 Hz and 3 kHz, which leads to think that the C1 sensitivity is dominated by "laser frequency noise" in this range of frequencies. In order to know what kind of "laser frequency noise" is involved, the two models given by equations **(3)** and **(5)** (cf. Section 4.1) have been tested. The results are presented in Figure 5. The normalisation factors used to plot the curves are : $K_{V®Hz} = 31.25 \times 10^{3}\ Hz.V^{-1}$ and $K_{V®m} = 3.33 \times 10^{-5}\ m.V^{-1}$. These values have been chosen in order to adjust the models to the sensitivity curve level and their order of magnitude is as expected.

The curve corresponding to the IMC length noise model suits very well to the sensitivity curve between 10 and 100 Hz, and also for bumps between 140 and 250 Hz. This means that IMC length noise limits the sensitivity in this range of frequencies. As a matter of fact, one of the main hypothesis to explain this noise is the effect of the IMC Automatic Alignment (AA) loop whose goal is to maintain the IMC end mirror aligned with respect to the Input Bench (IB) (see Figure 3). Supposing that an environmental noise (for example acoustic noise) excites the bench, the AA loop transmits this noise to IMC end mirror, which induces IMC length noise since angular motion is coupled with length displacements.

Between 100 Hz and 3 kHz, the model which suits better to the sensitivity corresponds to the IMC length control noise. This loop introduces a "readout noise" from the Reference Cavity reflection signal (which is called "Reference Cavity length noise" in [2]).

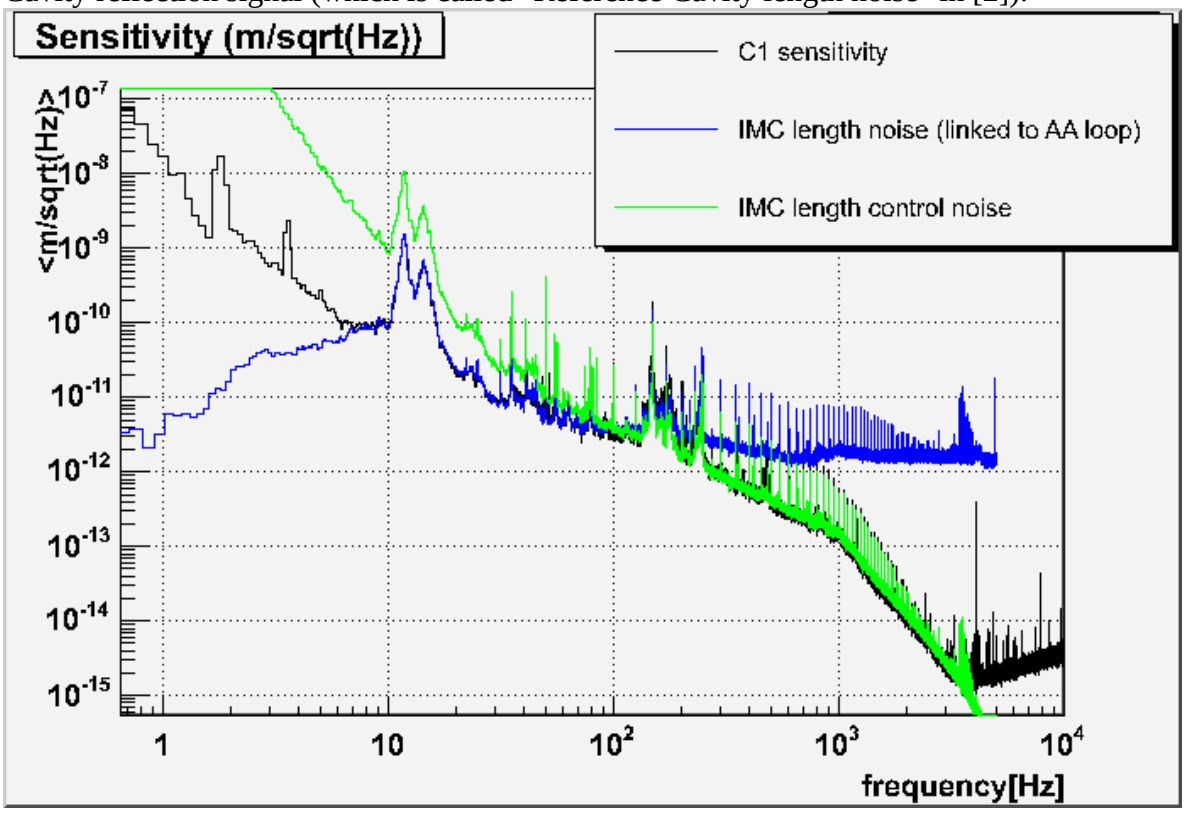

Figure 5 : *Models for "Laser frequency noise" compared to the sensitivity during C1*

4.3. "Laser frequency noise" during C2

Both gains of the IMC length control loop and of the IMC Automatic Alignment loop were lowed just before C2 run in order to decrease the "laser frequency noise" contribution in the sensitivity. After the reduction of the IMC control bandwidth, it has been shown in [3] that some coherence between the dark fringe signal and the IB z control was visible. So, IB x, y and z control were switched off in order to improve the sensitivity at low frequencies. The result of these modifications is shown in Figure 6 ; the curves were obtained with C2 data when North cavity was locked. The values chosen for the normalisation factors are : $K_{V®Hz} = 42 \times 10^{3}$ $Hz.V^{-1}$ and $K_{V®m} = 2.92 \times 10^{-5}$ $m.V^{-1}$. The value of $K_{V®Hz}$ corresponds exactly to the calibration of Sc_IB_zErrGC given in [4]. The value of $K_{V®m}$ is comparable to that used for C1.

In Figure 6, the IMC length noise model suits very well to the sensitivity curve between 1.5 and 30 Hz and for peaks between 35 and 80 Hz. The reduction of the IMC Automatic Alignment bandwidth made it possible to remove the two resonances between 10 and 20 Hz (see Figure 5). Nevertheless, below 10 Hz, "laser frequency noise" has increased, since control loops are less efficient to correct real angular motion noise of the Injection Bench. In fact, this angular noise seems to be introduced by IB angular local control since it has

been shown in [3] that the dark fringe signal is now coherent with channel Sc_IB_txCorr between 1.5 and 10 Hz.
Between 30 and 120 Hz, IMC length control noise still dominates the sensitivity but it is lower than during C1 thanks to the reduction of the IMC length control bandwidth : This way the "readout noise" is not reintroduced.

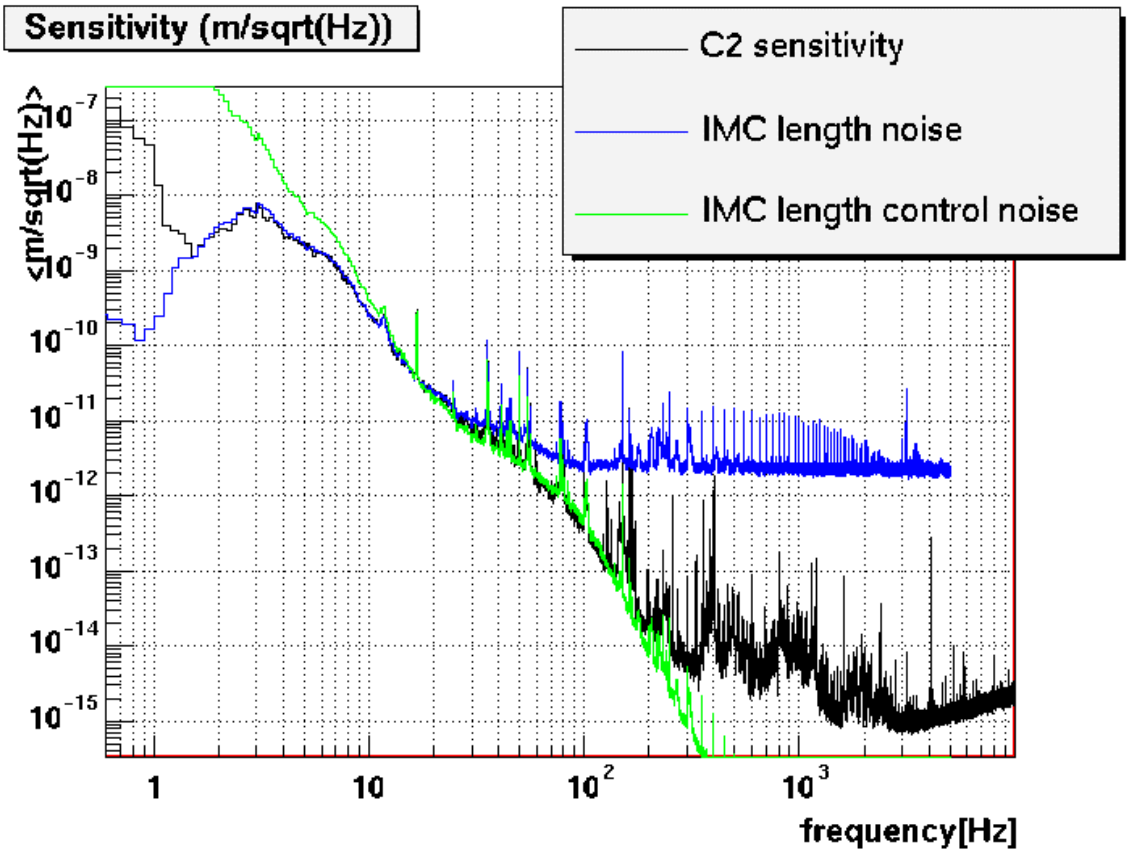

Figure 6 : *Models for "laser frequency noise" compared to the sensitivity during C2*

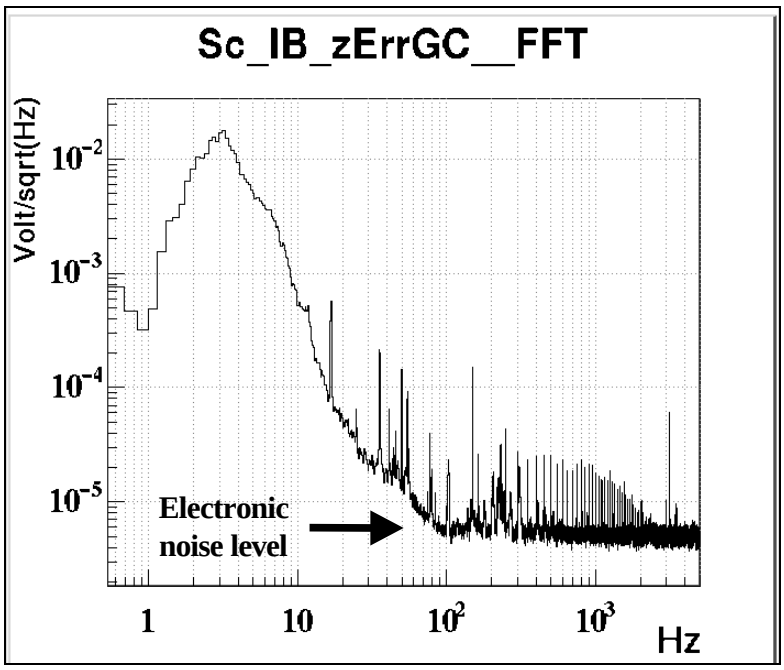

Figure 7 : *Amplitude spectrum of the Reference Cavity reflection signal during C2*

What is new in the C2 sensitivity is that the noise between 120 Hz and 3 kHz cannot be explained by the "laser frequency noise" models developed in section 4.1. Nevertheless, as the Reference Cavity reflection signal Sc_IB_zErrGC was limited by electronic noise during C2 above 100 Hz (see Figure 7), we cannot exclude that "laser frequency noise" still limits the sensitivity at these frequencies. Other hypothesis for noise sources will be discussed in the following.

5. Source of noise between 120 Hz and 3kHz during C2

The source of noise between 120 Hz and 3 kHz during C2 has been looked for. First the hypothesis of power noise has been made (section 5.1). It was then found that the scroll pumps vibrations have an impact on the sensitivity in this frequency range (section 5.2).

5.1. Power noise hypothesis

In order to understand how the Interferometer (ITF) signal (Pr_B1p_ACp or Pr_B1_ACp) can become sensitive to power fluctuations, we will first consider the ideal conditions for which the beam would be composed of only one TEM mode (the TEM 00). In this case, power fluctuations cannot affect the ITF signal when the length of the Fabry-Perot (FP) cavity strictly verifies the resonance condition : It corresponds to an extremum for Pr_B1(p)_DC and a zero for the demodulated signal Pr_B1(p)_ACp (therefore the resonance condition is analogous to a dark fringe condition). Now, let's suppose that the FP cavity is not exactly locked on the B1(p) dark fringe and note DL_{arm} the gap between the real length of the FP cavity and the length which corresponds to the dark fringe. In this case, the amplitude S of the demodulated signal is linked to DL_{arm} and to the DC power P by the relation :

$$S \mu P \times DL_{arm} \qquad \textbf{(6)}$$

DL_{arm} is the sum of two contributions : $DL_{arm} = DL_0 + dL$ **(7)**

DL_0 is the static length gap due to the fact that the FP cavity is not exactly locked on the dark fringe. dL symbolises length fluctuations of the FP cavity (which could be induced by the effect of a gravitational wave for example).

P can be decomposed in the same way : $P = P_0 + dP$ **(8)**

P_0 is the mean DC power and dP symbolises power fluctuations.

If equation **(6)** is developed to the first order by using relations **(7)** and **(8)** :

$$S \mu P_0 \times DL_0 + P_0 \times dL + dP \times DL_0 \qquad \textbf{(9)}$$

The third term in equation (9) shows that the difference DL_0 between the length which corresponds to the lock of FP cavity and the length which verifies the resonance condition of the TEM 00 is responsible for the ITF signal sensitivity to power fluctuations. The resulting power noise converted in m/√Hz is obtained from the relation :

$$dL = DL_0 \times dP/P_0 \qquad \textbf{(10)}$$

If the beam is composed only of the TEM 00 mode, DL_0 would be due to an electronic offset and would probably be negligible. But in more realistic conditions, the FP cavity is locked on an "average dark fringe" taking into account all TEM modes. So, in this case, DL_0 represents the difference between the length of the cavity locked on this "average dark fringe" and the length of the cavity which would minimise the sensitivity of the TEM 00 mode to power fluctuations.

Figure 8 shows a gap of about 1.5 mW between Pr_B1_ACp and Pr_B1p_ACp. It is due to the fact that the dark fringe condition differs between these two signals as the beam B1p is taken before the Output Mode Cleaner and contains a larger proportion of TEM modes of higher orders. DL_0 is evaluated by considering that it has the same order of magnitude as the gap between B1 and B1p signals, converted in meters thanks to the calibration optical gain. We find :

$$DL_0 \approx 2.6 \times 10^{-10}\ m \qquad \textbf{(11)}$$

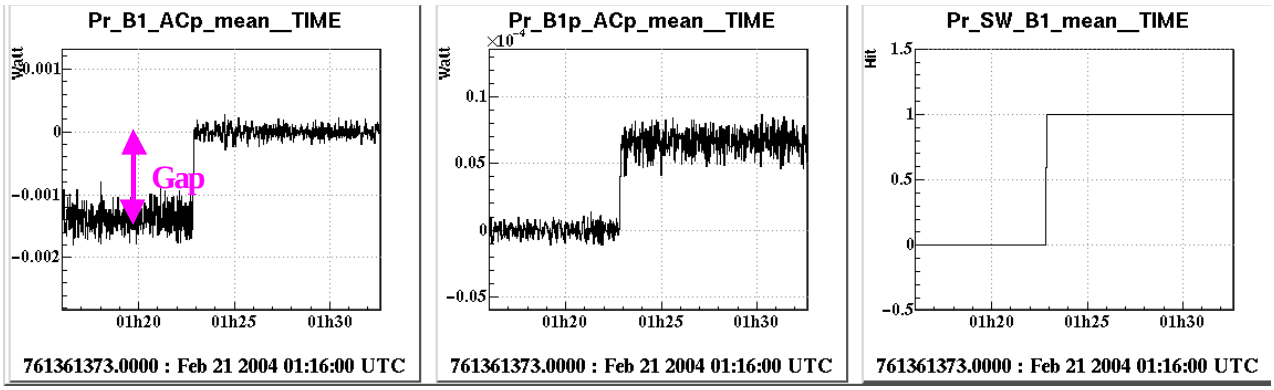

Figure 8 : *Gap between Pr_B1_ACp and Pr_B1p_ACp observed when the control of the cavity is switched from B1p to B1*

The relative power fluctuation is estimated from the signal transmitted by the IMC (Sc_IB_TraMC) :

$$\frac{dP}{P_0} = \frac{FFT(Sc\_IB\_TraMC)}{Mean(Sc\_IB\_TraMC)} \qquad \textbf{(12)}$$

Mean(Sc_IB_TraMC) is the average value of Sc_IB_TraMC.
The power noise contribution to the sensitivity curve during C2 has been evaluated thanks to the relations **(10)**, **(11)** and **(12)**. The result is shown in Figure 9.

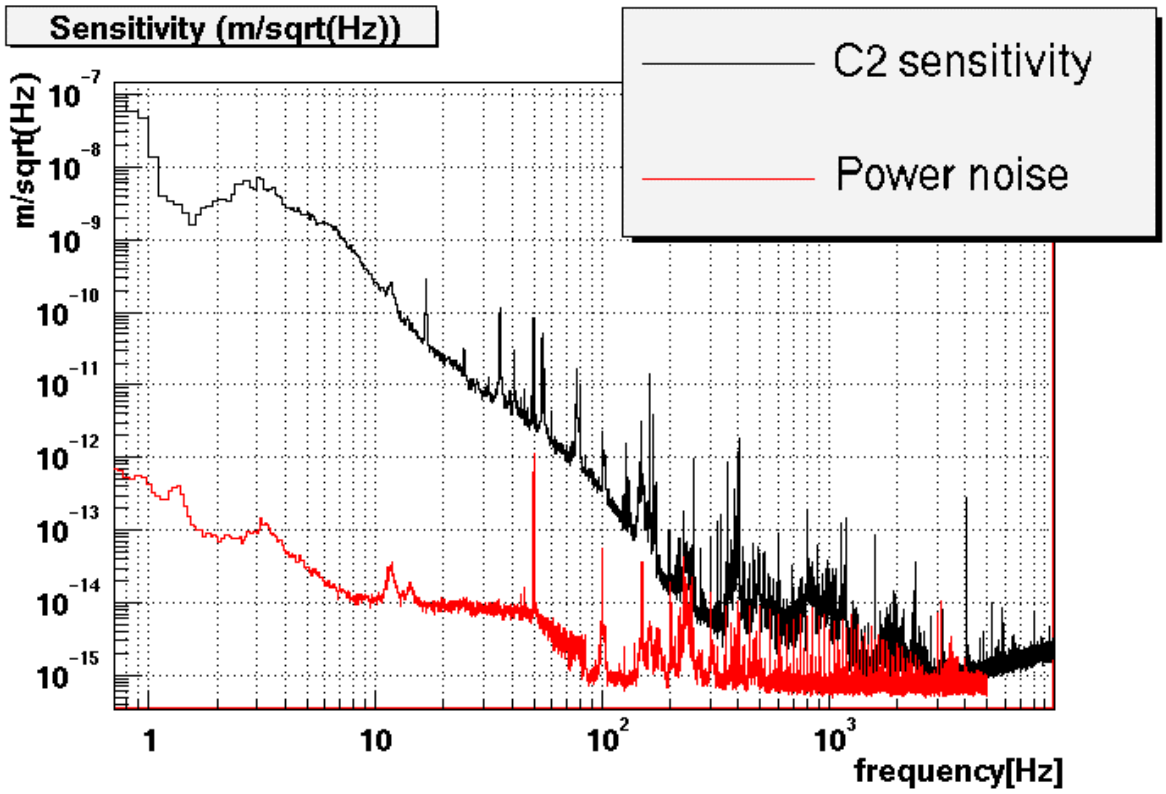

Figure 9 : *Power noise model compared to the sensitivity during C2*

The power noise model does not suit to the sensitivity curve. Even in the 230-250 Hz region where both sensitivity and power noise present a bump, there is more than a factor of five between the two curves. Thus, power noise does not seem to limit the C2 sensitivity. This conclusion is confirmed by Figure 10, where the sensitivity curve obtained when the FP cavity was locked on the dark fringe of B1 is compared to the sensitivity obtained when the cavity was locked on the dark fringe of B1p. In both cases, the sensitivity has been evaluated from the channel Pr_B1_ACp. If the sensitivity was limited by power noise in the 120 Hz - 3kHz region, the noise level when lock is obtained from B1p signal should be higher, since B1p contains a larger proportion of TEM modes of superior orders. But the two curves of Figure 10 overlap very well.

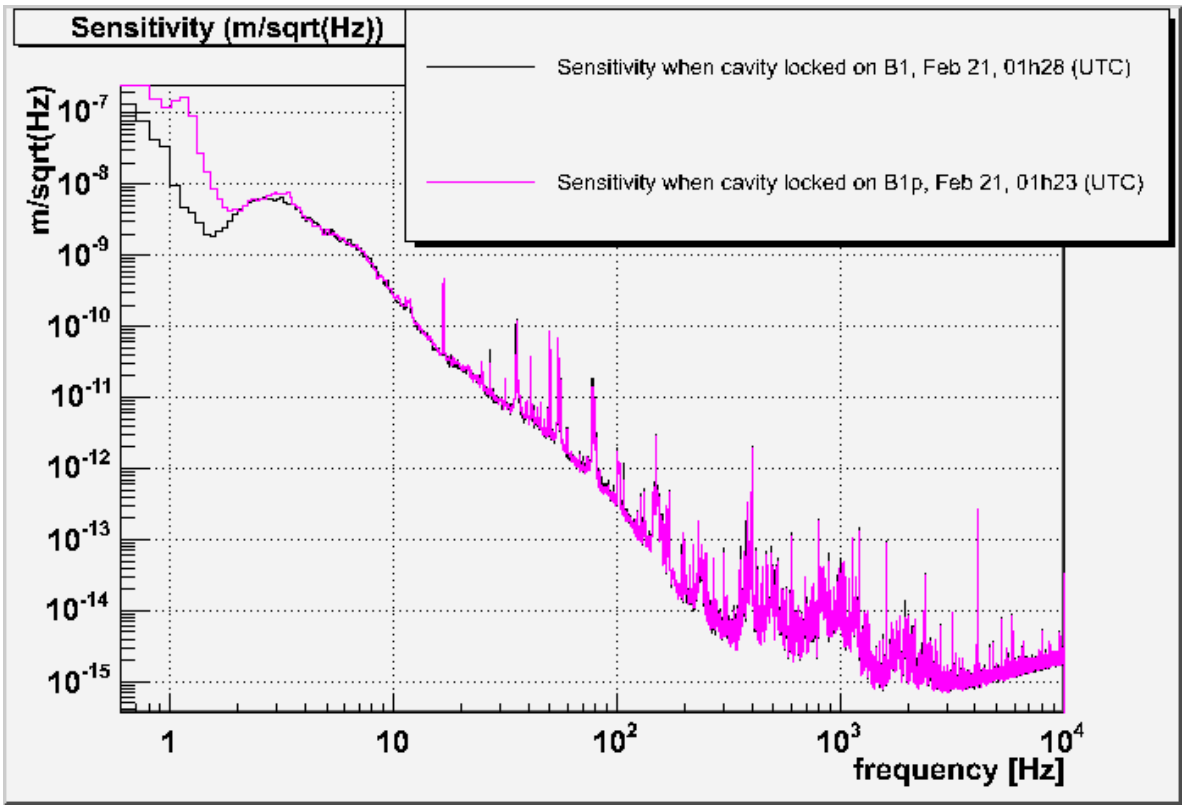

Figure 10 : *Two sensitivity curves compared : when lock uses B1 or when lock uses B1p*

5.2. Scroll pumps effect

Since power noise does not limit the sensitivity between 120 Hz and 3 kHz, we have to look for another source of noise. By looking at the time-frequency graph of the dark fringe signal obtained from C2 data, we can observe that the noise level decreases for about one hour on Saturday, February 21st 2004 (between 14h00 and 15h00 UTC, see Figure 11). At this time, all scroll pumps were progressively switched off, except MC pump which was already off. IB scroll pump was switched off at 14h00, exactly when the noise is the more reduced. Consequently it seems obvious that scroll pumps (and especially IB pump) vibrations are noise sources for the interferometer. In order to precise what frequency region is the most affected by this effect, we have compared in Figure 12 the sensitivity curve obtained when all scroll pumps are off (at 14h30 UTC) and the sensitivity curve obtained with original conditions restored (at 15h10 UTC). One can notice that scroll pumps activity has a visible impact on the sensitivity between 200 Hz and 1.5 kHz, so this noise contributes to the sensitivity curve in the frequency range not explained by "laser frequency noise" models.

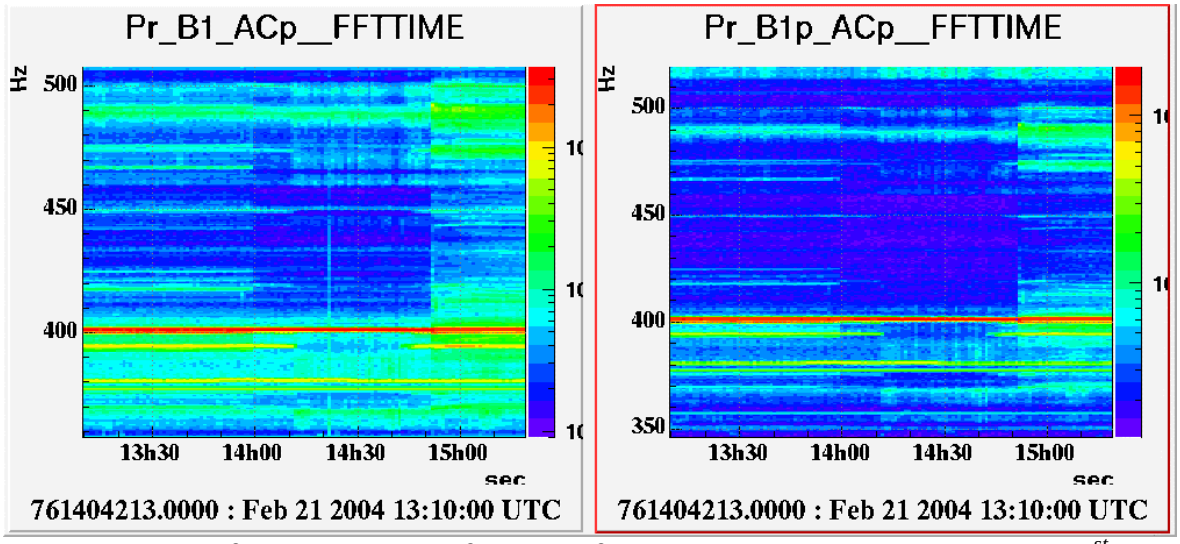

Figure 11 : *Time-frequency graph of the dark fringe signal on Saturday, February 21st 2004*

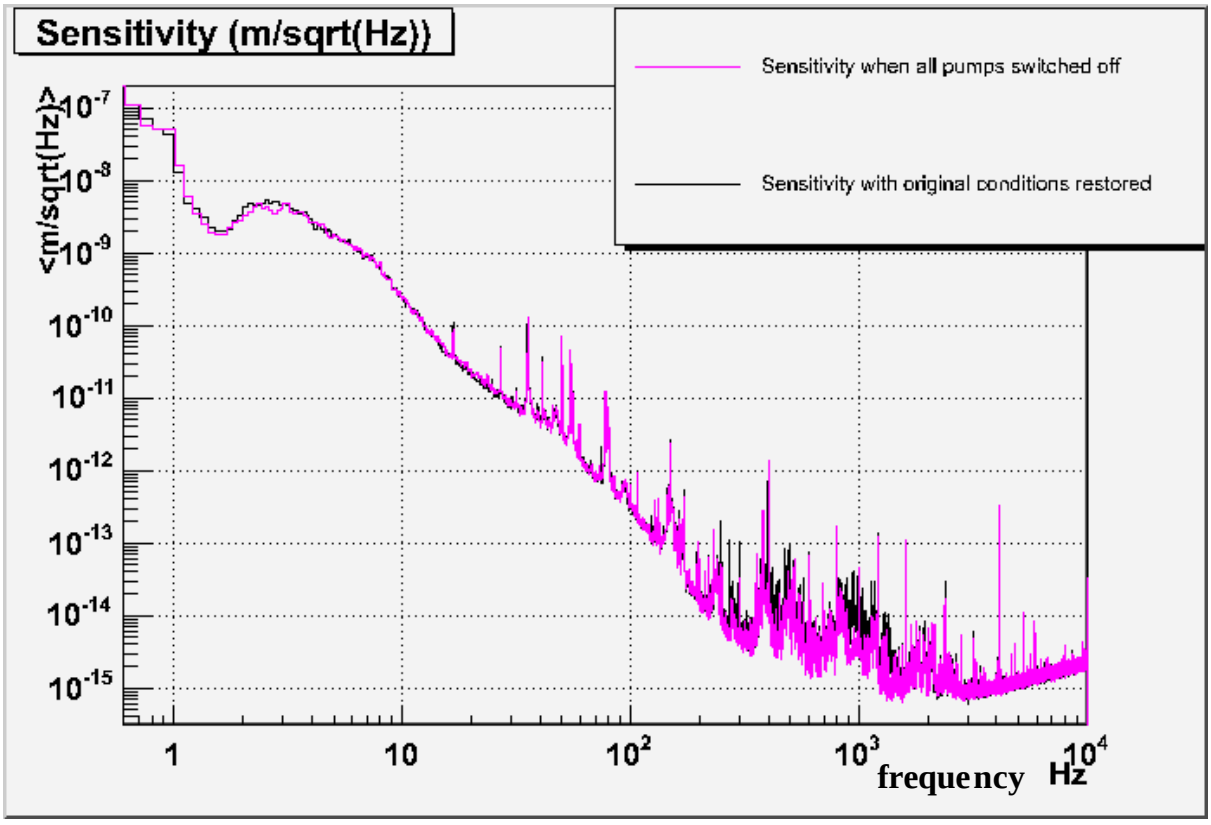

Figure 12 : *Sensitivity with scroll pumps ON compared to sensitivity with scroll pumps OFF during C2*

6. Angular motion noise

This section is devoted to the possible sources of noise at low frequencies (below 10 Hz for C1 and below 1.5 Hz for C2). First, it is shown in section 6.1 that low frequency peaks in the sensitivity curve are linked to mirror resonances. The effect of the North Input mirror angular control during C1 is presented in section 6.2.

6.1. Mirror resonances

Figure 13 shows a zoom at low frequencies on the sensitivity curve obtained during C1 from the channel Pr_B1_ACp. Some resonances have been indicated.

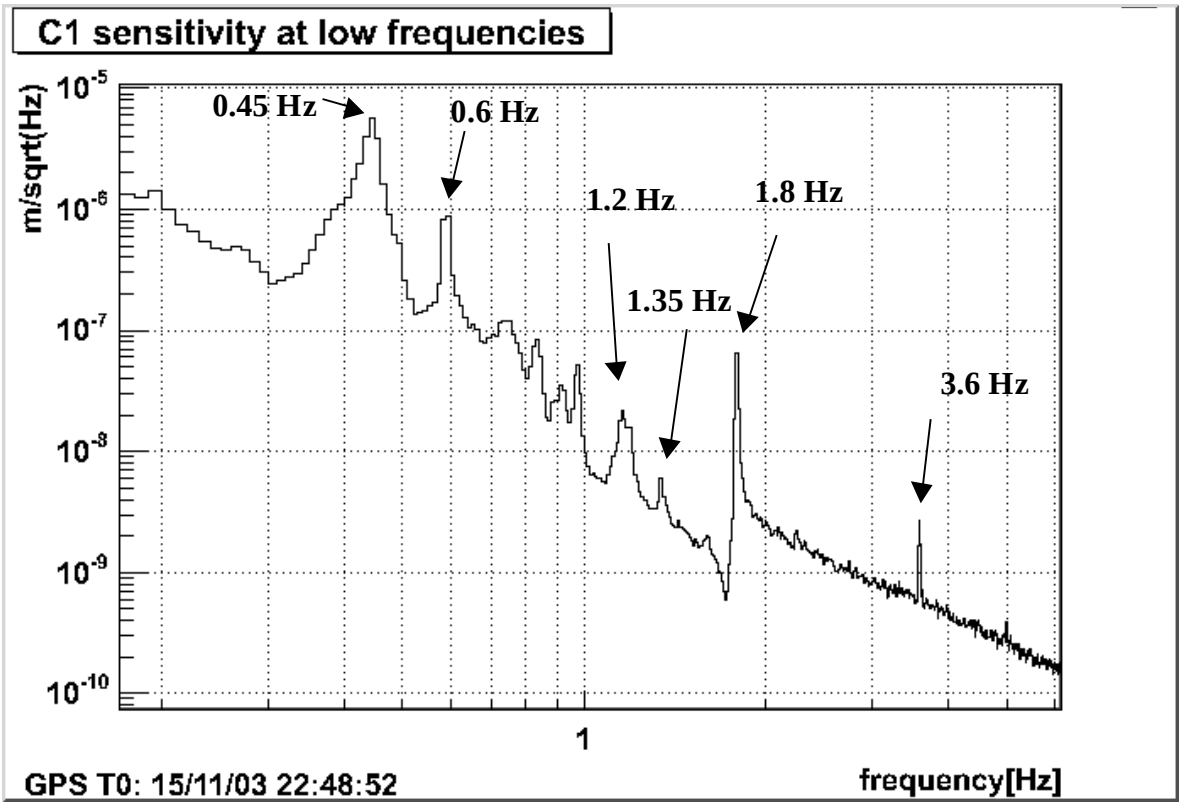

Figure 13 : *Mirror resonances in the C1 sensitivity when the lock of the cavity is controlled with the beam B1*

All these resonances are due to mirrors angular motion :

- The resonance at 0.45 Hz is visible in the amplitude spectrum of the signals which measure the angular position of the North Input (NI) and the North End (NE) mirrors in θx and θy.
- The resonance at 0.6 Hz is visible in the two angular degrees of freedom of NE mirror.
- The resonance at 1.2 Hz is due to an oscillation in θy and the resonance at 1.8 Hz is due to an oscillation in θx of both NI and NE mirrors.
- The resonance at 3.6 Hz is the double frequency of 1.8 Hz. The presence of double frequencies in the sensitivity curve is due to the fact that in ideal alignment conditions (when the average angular position corresponds to a maximum for the power stocked in

cavity), an angular displacement at a frequency *f* creates power fluctuations at a frequency of *2f*. In realistic conditions, the average angular position of the two mirrors NE and NI does not always corresponds to the maximum for power. So we find in the sensitivity a mixture between simple and double frequencies.

- The resonance at 1.35 Hz is observed in the spectrum of the square of [Gx_NE(I)_tx - Mean(Gx_NE(I)_tx)], where "Mean" is for the average value of the corresponding channel.

These examples prove that mirror oscillations have an impact on sensitivity at low frequencies.

6.2. *Angular noise*

During C1, a good coherence has been observed between the dark fringe signal and Sc_NI_txCorr (see Figure 14). This channel gives the correction signal sent to the marionette of the NI mirror to correct the angular position in θx.

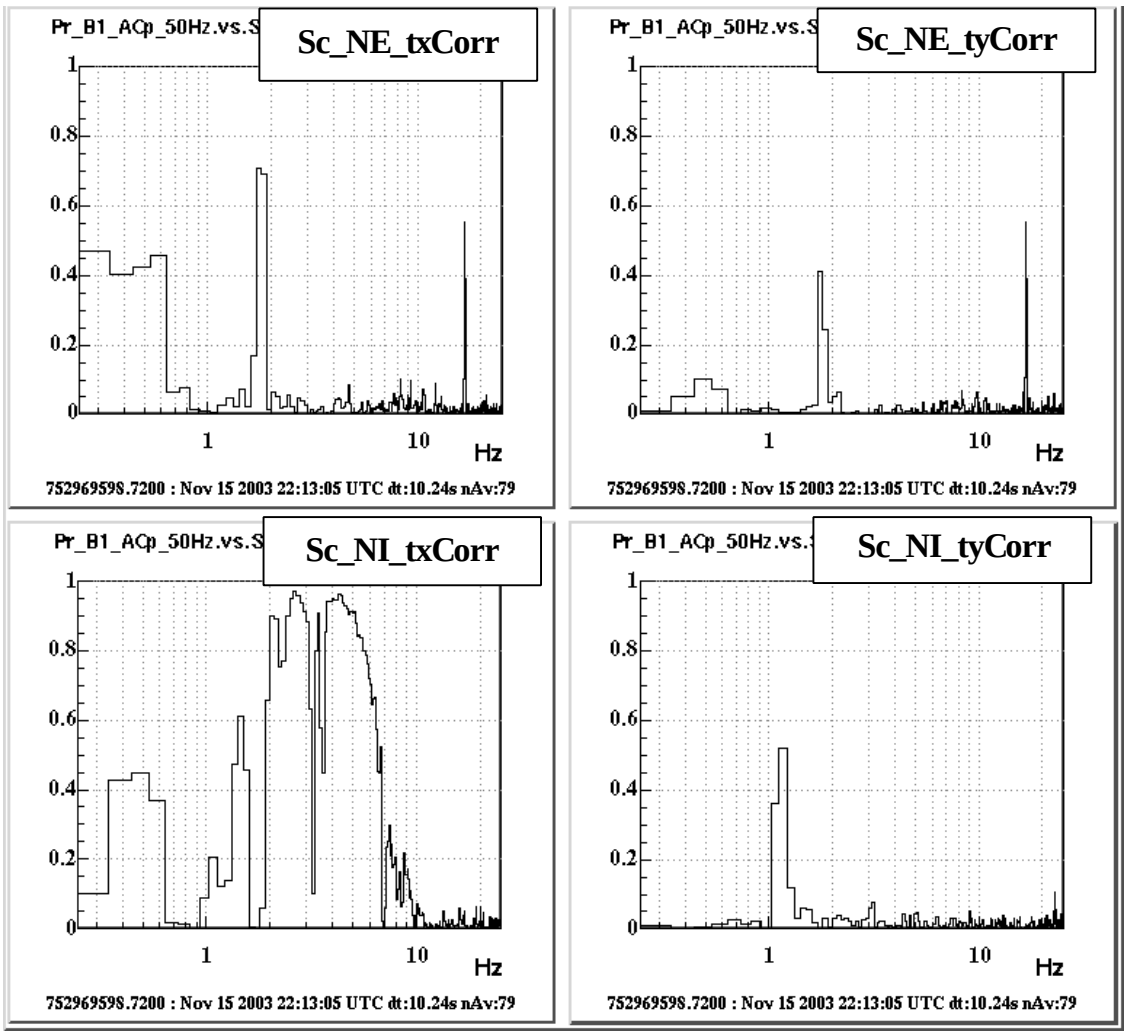

Figure 14 : *Coherences between the dark fringe signal and the correction signals sent to the marionettes of NE and NI mirrors during C1*

The curves of Figure 14 have been plotted at GPS time = 752968813 (November 15th 2003, 22h00 UTC) when north cavity was locked with Pr_B1_ACp. The coherence observed between the dark fringe signal and Sc_NI_txCorr is good during the 3 days of the run, except on Monday, November 17th, when north cavity is locked with Pr_B1_ACp (the reason is not understood).

Thus, we have looked for a model to propagate the noise injected by the local control in θx of the NI mirror through the interferometer. The simplified model we have retained can be wrote as :

$$dl = FFT(Sc\_NI\_txCorr) \times TF(excitation\ on\ marionette \rightarrow mirror\ position) \times K_0 \qquad \textbf{(13)}$$

where :

- *TF(excitation on marionette ® mirror position)* is the transfer function between the correction signal sent to the marionette and the angular position measured on the mirror :

$$TF(excitation\ on\ marionette \rightarrow mirror\ position) = \frac{FFT(Gx\_NI\_tx)}{FFT(Sc\_NI\_txCorr)} \qquad \textbf{(14)}$$

This transfer function has been calculated from one hour of data starting at GPS time = 751938106 (November 3rd 2003, 23h41 UTC). The result is presented in Figure 15.

- K_0 is a normalisation factor to convert the angular displacement given in μrad into a longitudinal displacement in meters.

Equation **(13)** gives a very approximate model since it supposes that the relation between the angular displacement and the sensitivity is linear, which is wrong : if one wanted to build a more precise model, it would be necessary to add a quadratic term to the model (in order to take into account the double frequencies). Nevertheless, the simplified model gives quite satisfying results (see Figure 16) as it suits very well to the sensitivity curve during C1, between 1.8 Hz and 6 Hz. The normalisation factor used to plot the curve is : $K_0 = 2.7 \times 10^{-8}$ *m.mrad*. This value has been chosen in order to adjust the model to the sensitivity curve level. If we try to calibrate the model using the period of data when a line at 5.4 Hz was injected into Sc_NI_txCorr (on November 17th, around 23h20 UTC), we find : $K_0 = 1.6 \times 10^{-8}$ *m.mrad*. Thus, the calibration does not work very well, but the period of data with the line was very noisy : A large seismic noise was responsible for a 300 mHz oscillation. This observation added to the fact that the model does not take into account the double frequencies can probably explain the difference between the two values of K_0.

In conclusion, one can assert that the C1 sensitivity is limited by angular noise (on NI mirror, in the θx degree of freedom) between 1.8 and 6 Hz. It is not possible to verify if the same correlation between the sensitivity and the correction signal Sc_NI_txCorr still exist during C2, since the "laser frequency noise" has increased at low frequencies and dominates the C2 sensitivity above 1.5 Hz.

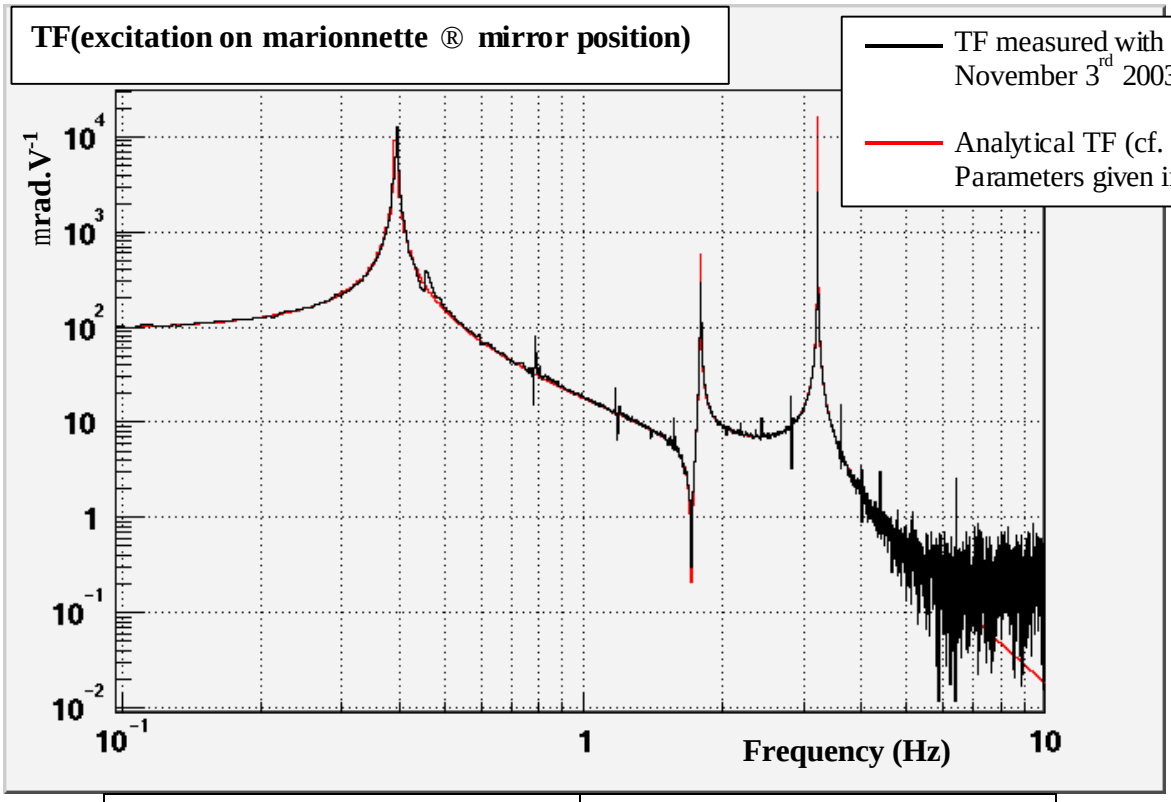

Poles		Zeroes	
Freq [Hz]	**Q**	**Freq[Hz]**	**Q**
0.392	30000	1.713	1000
1.794	10000		
3.215	10000		
DC gain		9.3×10^{1}	

Table 1 : *Parameters of the analytical transfer function*

Figure 15 : *Mechanical Transfer Function for NI mirror (in qx)*

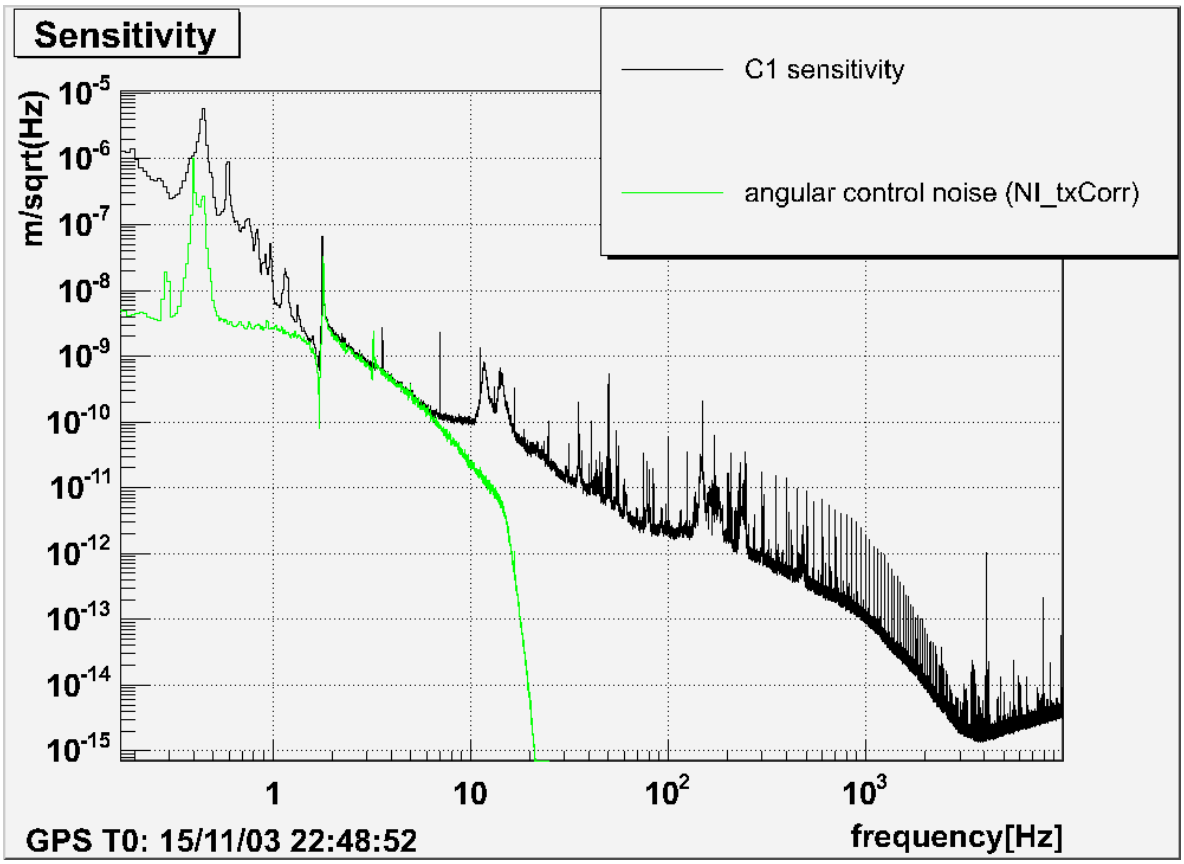

Figure 16 : *Model for angular control noise compared to the sensitivity during C1*

7. Comparison between North arm and West arm

Figure 17 shows the two sensitivity curves obtained during C2 when North cavity or West cavity were locked. The two curves are quite similar. Yet, contrary to the West cavity which was not automatically aligned, the North cavity was aligned thanks to the Linear Alignment. This should reduce mirror angular motion noise at low frequencies. Nevertheless, as the C2 sensitivity is limited by IMC length noise above 1.5 Hz, no improvement due to Linear Alignment can be seen.

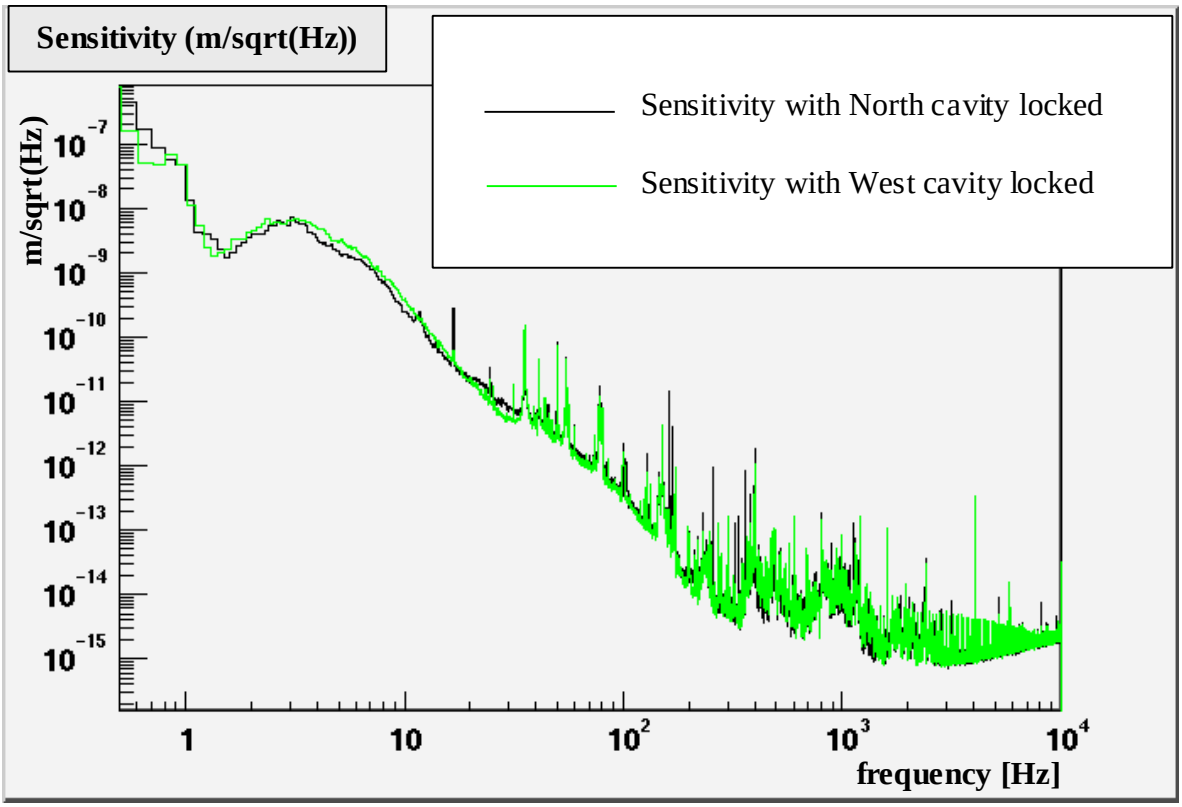

Figure 17 : *Comparison between North cavity and West cavity during C2*

8. Conclusions

Both C1 and C2 sensitivities are limited by electronic (ADC) noise above 3 kHz. This noise will be reduced by using compression filters to increase the dynamics of the electronics.
Between 10 Hz and 3 kHz, the sensitivity during C1 is limited by "laser frequency noise". Actually, this noise can be decomposed in two contributions : an IMC length noise between 10 Hz and 100 Hz (which mainly results from the transmission of an environmental noise by the Automatic Alignment loop) and an IMC length control noise (which is due to the fact that the channel Sc_IB_zErrGC(x30) contains some "readout noise"). Before C2 run, this "laser frequency noise" was lowed by reducing the IMC control bandwidth and by removing IB local control in x, y and z. However, the sensitivity during C2 is still dominated by IMC length noise between 1.5 and 30 Hz, and by IMC length control noise between 30 and 120 Hz. The contribution in the sensitivity of "Laser frequency noise" should be reduced with the Michelson recombination and with the second stage of laser frequency stabilisation.
During C2 run, the sensitivity is not clearly explained between 120 Hz and 3 kHz. It has been shown that scroll pumps vibrations have an impact on the sensitivity but the propagation model of this noise is not known. The contribution of "laser frequency noise" cannot be excluded because the Reference Cavity reflection channel is limited by electronic noise above 100 Hz. On the other hand, the hypothesis of power noise has not been confirmed.

At low frequency (below 10 Hz) the sensitivity during C1 is limited by mirrors angular motion noise below 10 Hz, but it cannot be verified for the C2 sensitivity since IMC length noise dominates low frequencies.
The sensitivities obtained with North cavity and West cavity during C2 are identical.

9. References

[1] R. Flaminio. *Laser frequency noise generation and propagation during C1 (preliminary).*
http://wwwcascina.virgo.infn.it/commissioning/C1/InvestigationsDocuments/Readout_noise/C1meeting_laser_noise.ppt, December 2003.

[2] F. Bondu. *Phase Modulation due to the Motion of the Input Mode Cleaner Mirrors in C1 Configuration.* Virgo Note VIR-NOT-OCA-1390-260, February 2004.

[3] H. Heitmann, G. Losurdo, R. Flaminio. *Laser frequency noise reduction.*
http://wwwcascina.virgo.infn.it/commissioning/weekly/Feb2004/Weekly10Feb2004.ppt, February 2004.

[4] H. Heitmann. *Calibration of Sc_IB_zErrGC.* Logbook entry - Injection System - Operation - Mon Jan 26 18:17:06 2004, GPS : 759172626.